Mon. Not. R. Astron. Soc. **000**, 000–000 (0000) Printed 1 February 2008 (MN LATEX style file v1.4)

Metallicities and kinematics of G and K dwarfs

Chris Flynn[1,3] and Olof Morell[2,4]
[1] *Tuorla Observatory, Piikkiö, FIN-21500, Finland*
[2] *Uppsala Observatory, Box 515, Uppsala, S-751 20, Sweden*
[3] *cflynn@astro.utu.fi*
[4] *olle.morell@helax.se*

Accepted, Received ; in original form

Key words: G and K dwarfs – abundances, kinematics

ABSTRACT

We have used accurate, spectroscopically determined abundances for G and K dwarfs of Morell, Källander and Butcher (1992) and Morell (1994), to derive a photometric abundance index for G and K dwarfs. Broadband Cousins $R-I$ photometry is used to estimate effective temperature and the Geneva b_1 colour to estimate line blanketing in the blue and hence abundance. Abundances can be derived in the range $-2.0 <$[Fe/H]< 0.5 for G0 to K3 dwarfs, with a scatter in [Fe/H] of 0.2 dex. We apply the method to a sample of Gliese catalog G and K dwarfs, and examine the metallicity and kinematic properties of the stars. The stars show the well established observational features of the disk, thick disk and halo in the solar neighbourhood. We find that the distribution of local K dwarf metallicity is quite similar to local G dwarfs, indicating that there is a "K-dwarf" as well as a G-dwarf problem.

1 INTRODUCTION

The distribution of metallicity in nearby G-dwarfs, a major constraint on models of the evolution of the Galaxy, has long presented us with the "G dwarf problem" (Pagel and Patchett 1975). The G-dwarf problem arises because there is an apparent paucity of metal poor G-dwarfs relative to what we would expect from the simplest (closed box) models of Galactic chemical evolution. There are rather a large number of ways that the evolutionary models can be modified in order to bring them into consistency with the data, such as pre-enrichment of the gas, a time dependent Initial Mass Function or gas infall.

G-dwarfs are sufficiently massive that some of them have evolved away from the main sequence, and these evolutionary corrections must be taken into account when determining their space densities and metallicities. While these problems are by no means intractable, it has long been recognised that K dwarfs would make for a cleaner sample of the local metal abundance distribution, because for these stars the evolutionary corrections are negligible. K dwarfs are of course intrinsically fainter, and it has not been until recently that accurate spectroscopic K dwarf abundance analyses have become available, with which to calibrate a photometric abundance estimator. Furthermore, with the release of *Hipparcos* data expected soon, accurate parallaxes and distances of a complete and large sample of K dwarfs will become available, from which the distribution of K dwarf abundances can be measured. Also, the accurate parallax results given by *Hipparcos* will mean that we can select dwarfs by absolute magnitude, which is a better way of isolating stars of a given mass range than is selection by colour (as has been used in samples of G dwarfs).

In this paper, we have developed a photometric abundance indicator for G and K dwarfs. In section 1 we have taken a sample of nearby disk G and K dwarfs for which accurate spectroscopic abundances in a number of heavy elements and effective temperatures have been measured by Morell (1994). We have supplemented these data with several low metallicity G and K dwarfs for which accurate metallicity and effective temperature data are available in the literature. In sections 2 and 3 we use broadband VRI and Geneva photometry (taken from the the literature), to develop an abundance index which correlates well with the spectroscopic metallicities, and can be transformed to abundance with an accuracy of circa 0.2 dex. In section 4 we measure abundances for approximately 200 G and K dwarfs drawn from the Gliese catalog. In sections 5 and 6 we describe the kinematics of the dwarfs, and demonstrate that the K dwarfs show the same paucity of metal deficient stars as seen in the G dwarfs, indicating that there is a "K dwarf" as well as a G dwarf problem. In section 6 we draw our conclusions.

2 SPECTROSCOPIC G AND K DWARF SAMPLE

Our starting point for calibrating a photometric abundance index for the G and K dwarfs is a sample of accurate and homogeneously determined spectroscopic abundances. Good abundances for K dwarfs have been difficult to carry out until recently, because of the effects of line crowding, the extended damping wings of strong lines, the strong effects on the atmospheres of molecular species and the intrinsic faintness of the stars.

Our sample of dwarfs comes primarily from Morell, Källander and Butcher (1992) and Morell (1994). These authors give accurate metallicities, gravities and effective temperatures for 26 G0 to K3 dwarfs. Morell (1994) observed a sample of dK stars with high dispersion (resolving power 90,000) and high signal to noise with the ESO Coudé Auxiliary Telescope (CAT) at La Silla. The sample included all dK stars in the Bright Star Catalogue which were observable from La Silla, after removing known spectroscopic binaries. Wavelength regions were primarily chosen to determine CNO abundances as well as various metals (Na, Mg, Al, Si, Ca, Sc, Ti, V, Cr, Fe, Co, Ni, Cu, Y, Zr, La, Nd) at 5070.0 to 5108.0 Å, 6141.0 to 6181.5 Å, 6290.0 to 6338.0 Å, 6675.0 to 6724.5 Åand 7960.0 to 8020.0 Å. Signal to noise exceeded 100 for most stars and spectral regions.

The spectra were analysed using spectral synthesis methods, based on model atmospheres calculated with the ODF version of the MARCS program (Gustafsson et. al. 1975). Initial estimates of the stellar effective temperatures were made from the $V-R$ and $R-I$ colours, using the temperature scale of vandenBerg and Bell (1985). (Cousins UBVRI photometry was obtained for 17 stars with the ESO 50 cm telescope in April and November 1988 and February 1989). The temperatures were then improved by examining 12 Fe lines with a range of excitation energies, and adjusting the temperatures until no trends were seen between excitation energy and the derived abundance of the species. For half the stars this lead to adjustments of less than 50 K, and for the remaining half to adjustments between 50 and 250 K. Gravities were determined from a single Ca line at $\lambda\,6162$ Å. Three of the G stars in the sample were found to be slightly evolved, with lower log(g) values. Abundances were determined using spectral synthesis techniques for many species; here we describe only the Fe abundances. Fe abundances were measured for 12 neutral, weak and unblended Fe lines, and very good agreement was obtained amongst the lines. The errors in the derived mean Fe abundances are estimated as smaller than 0.05 dex. An error of approximately 100 K in adopted effective temperature leads to a change in derived Fe abundance of only 0.01 dex, so any systematic errors in the temperature scale do not have a large effect on the abundance scale. Table 1 shows our sample of G and K dwarfs. Column 1 shows the HD number, column 2 a secondary identification, column 3 the spectral type Sp, column 4 the effective temperature $T_{\rm eff}$, column 5 the surface gravity log(g), and column 6 the spectroscopically determined abundance $[{\rm Fe/H}]_{\rm Spec}$, with a note on its source in column 7. Columns 8 and 9 show b_1 and Cousins $R-I$, with a note on the source of $R-I$ in column 10. The estimated abundance $[{\rm Fe/H}]_{\rm Gen}$ based on b_1 and $R-I$ (as described in the next section) is shown in last column.

In the next section we develop a photometric abundance index for G and K dwarfs, which correlates well with the spectroscopic abundances determined above. Our aim was to find such an index over as wide a range of metallicity as possible, so we have supplemented the Morell data (which are almost all relatively metal rich disk stars) with a small number of metal weak stars for which spectroscopic metallicities and effective temperatures have been determined from high dispersion spectral analyses. These stars were found by searching for metal weak G and K dwarf stars in the "Catalog of [Fe/H] Determinations" (Cayrel de Strobel et. al. 1992), with high dispersion abundance analyses, and for which Cousins $R-I$ and Geneva photometry could be located in the literature. The stars are shown in the last 9 rows of table 1, and come mostly from Rebolo, Molaro and Beckman (1988). Sources of all the spectroscopic and photometric data are shown below the table.

3 ABUNDANCE AND EFFECTIVE TEMPERATURE CALIBRATION

In order to qualitatively understand the effects of [Fe/H] and $T_{\rm eff}$ on K dwarfs, a set of synthetic spectra of K dwarf stars over a grid of [Fe/H] and $T_{\rm eff}$ was kindly prepared for us by Uffe Gråe Jørgensen. As expected, the main effects of metallicity could be seen in the blue regions (3000 to 4500 Å) where line blanketing is readily apparent.

For all our stars Geneva $(u, b_1, b_2, v_1, v_2, g)$ intermediate band photometry colours were available in the Geneva Photometric Catalog (Rufener 1989). Since Geneva photometry is available for a very large number of nearby G and K dwarfs, our initial attempt was to develop a photometric calibration based on Geneva colours only. However, it turned out that we could not reliably enough estimate effective temperature using Geneva photometry, which led to corresponding uncertainties in the abundance indices we developed. In the end we used broadband Cousins RI photometry to estimate effective temperatures, and the Geneva b_1 colour to define an index which measures line blanketing in the blue and correlates well with the spectroscopic abundances.

For various plausible colour indices c_i say, being linear combinations of the six Geneva $(u, b_1, b_2, v_1, v_2, g)$ colours, we found we could fit linear relations of the form

$$c_i = f_i\,[{\rm Fe/H}]_{\rm Spec} + t_i\;T_{\rm eff} + a_i. \qquad (1)$$

with low scatter (i.e. less than few×0.01 mag.), where f_i, t_i and a_i are constants. For any two such indices, c_1 and c_2 say, two relations can be inverted to derive a calibration for [Fe/H] and $T_{\rm eff}$. (Note that we also checked for dependence of each index on $\log(g)$, but no significant dependence was present for any of the indices tried. Hence we only consider $T_{\rm eff}$ and [Fe/H] here). We searched for two indices which were respectively more sensitive to abundance and to temperature, so the inversion would be as stable as possible. However, for all the filter combinations we tried, the linear relations fitted were close to being parallel planes, which is to say that in the spectral region covered by Geneva photometry, it is difficult to break the degeneracy between abundance and effective temperature effects for this type of star.

Moving to photometry in the near IR was the obvious way around this problem, since line blanketing is much

Table 1. The G and K dwarf sample.

HD	Other ID	Sp	$T_{\rm eff}$	log(g)	$[{\rm Fe/H}]_{\rm Spec}$	Note	b_1	$R-I$	Note	$[{\rm Fe/H}]_{\rm Gen}$
2151	HR98	G2IV	5650	4.0	−0.30	1	1.072	0.339	9	−0.33
4628	HR222	K2V	5150	4.6	−0.40	2	1.252	0.443	2	−0.18
10361	HR487	K5V	5100	4.6	−0.28	2	1.235	0.451	2	−0.42
10700	HR509	G8V	5300	4.4	−0.50	1	1.129	0.385	9	−0.45
13445	HR637	K1V	5350	4.6	−0.24	2	1.186	0.420	2	−0.43
23249	HR1136	K0IV	4800	3.9	−0.10	1	1.263	0.435	9	0.02
26965	HR1325	K1V	5350	4.6	−0.30	2	1.198	0.419	2	−0.31
38392	HR1982	K2V	4900	4.6	−0.05	2	1.301	0.462	2	−0.02
63077	HR3018	G0V	5600	4.0	−1.00	1	1.016	0.360	9	−1.06
72673	HR3384	K0V	5200	4.6	−0.35	2	1.157	0.405	2	−0.47
100623	HR4458	K0V	5400	4.6	−0.26	2	1.183	0.412	2	−0.35
102365	HR4523	G5V	5600	4.1	−0.30	1	1.080	0.360	9	−0.53
131977	HR5568	K4V	4750	4.7	0.05	2	1.420	0.522	2	0.20
136352	HR5699	G4V	5700	4.0	−0.40	1	1.073	0.350	9	−0.46
136442	HR5706	K0V	4800	3.9	0.35	2	1.372	0.473	2	0.43
146233	HR6060	G2V	5750	4.2	0.00	1	1.092	0.335	9	−0.11
149661	HR6171	K2V	5300	4.6	0.01	2	1.214	0.397	2	0.10
153226	HR6301	K0V	5150	3.8	0.05	2	1.260	0.450	2	−0.20
160691	HR6585	G3IV/V	5650	4.2	−0.10	1	1.124	0.335	9	0.15
165341	HR6752A	K0V	5300	4.5	−0.10	1	1.228	0.455	9	−0.53
190248	HR7665	G7IV	5550	4.4	0.20	1	1.171	0.345	9	0.41
192310	HR7722	K0V	5100	4.6	−0.05	2	1.255	0.419	2	0.16
208801	HR8382	K2V	5000	4.0	0.00	2	1.300	0.460	2	0.00
209100	HR8387	K4/5V	4700	4.6	−0.13	2	1.382	0.510	2	0.04
211998	HR8515	F2V:	5250	3.5	−1.40	1	1.033	0.410	9	−1.56
216803	HR8721	K4V	4550	4.7	−0.20	2	1.413	0.530	2	0.04
64090	BD+31 1684	sdG2	5419	4.1	−1.7	4	1.013	0.41	7	−1.72
103095	BD+38 2285	G8Vp	4990	4.5	−1.4	5	1.106	0.437	8	−1.30
132475	BD−21 4009	G0V	5550	3.8	−1.6	7	0.982	0.38	7	−1.60
134439	BD−15 4042	K0/1V	4850	4.5	−1.57	6	1.118	0.447	9	−1.33
134440	BD−15 4041	K0V:	4754	4.1	−1.52	6	1.185	0.478	9	−1.17
184499	BD+32 3474	G0V	5610	4.0	−0.8	7	1.032	0.36	7	−0.93
201889	BD+23 4264	G1V	5580	4.5	−1.1	7	1.031	0.37	7	−1.06
216777	BD−08 5980	G6V	5540	4.0	−0.6	7	1.079	0.38	7	−0.80
—	BD+29 366	—	5560	3.8	−1.1	7	1.010	0.39	7	−1.49

1 : Morell, Källander and Butcher (1992)
2 : Morell (1994)
3 : Spite, Spite, Maillard (1984)
4 : Gilroy et.al. (1988), Peterson (1980), Rebolo, Molaro and Beckman (1988)
5 : Sneden and Crocker (1988)
6 : Petersen (1980), Carney and Petersen (1980) and Petersen (1981)
7 : Rebolo, Molaro and Beckman (1988)
8 : Taylor (1995)
9 : Bessell (1990)

weaker in this region. We gathered VRI photometry from the literature for the stars, and experimented with the colour indices $V-R$ and $R-I$ (R and I are throughout the paper on the Cousins system). The $R-I$ data are shown in the last column of table 1, and are primarily from Morell (1994) and Bessell (1990). $R-I$ turned out to have no measurable dependence on the metal abundance of the stars, and could be used as a very robust temperature estimator, whereas $V-R$ still showed some dependency on metallicity. We tried combinations of $R-I$ and Geneva colours and found that $R-I$ and b_1 gave an index which correlated best with the spectroscopic abundances. (All the Geneva colours were found to measure line blanketting in the blue and correlated with metallicity to some extent, with the lowest scatter being for b_1). The relations we fit are:

$$R-I = 1.385 - \ T_{\rm eff}/5413.5 \tag{2}$$

$$b_1 = 0.121\,[{\rm Fe/H}]_{\rm Spec} - \ T_{\rm eff}/3480.7 + 2.737. \tag{3}$$

The scatter around the fits Δb_1 and $\Delta(R-I)$ are shown as functions of $[{\rm Fe/H}]_{\rm Spec}$, $T_{\rm eff}$, log(g), b_1 and $R-I$ in Figure 1. There are no apparent systematic residuals in the fitting as functions of any of these quantities. In particular, in the case of $R-I$, there is no dependance on $[{\rm Fe/H}]_{\rm Spec}$ or log(g), although neither was explicitly fitted, and in the case of b_1, there is no dependence on log(g), although this was not explicitly fitted.

Inverting these relations, we derive :

$$T_{\rm eff} = 7494. - 5412.\,(R-I) \tag{4}$$

$$[{\rm Fe/H}]_{\rm Gen} = 8.248\,b_1 - 12.822\,(R-I) - 4.822 \tag{5}$$

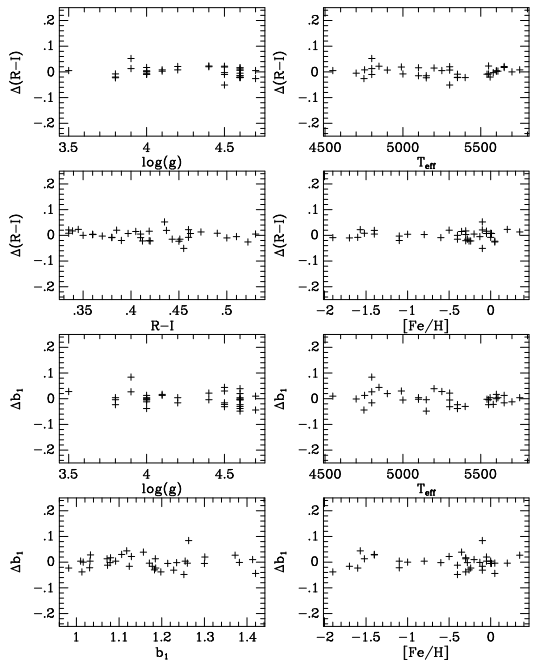

Figure 1. The scatter in the fits to b_1 and $R-I$ (Δb_1 and $\Delta(R-I)$ respectively) is shown as functions of $T_{\rm eff}$, [Fe/H], log(g), b_1 and $R-I$. There are no apparent residual trends in the fits in any of these quantities.

Eqns (4) and (5) are valid in the range $0.33 \leq R-I \leq 0.55$, which corresponds roughly to G0 to K3 dwarfs.

Effective temperature calibrations for the $R-I$ filter have been made by Bessell, Castelli and Plez (1996) from synthetic spectra and filter band passes, and by Taylor (1992) who used model atmosphere analyses of Balmer line wings. We show in Figure 2 Bessell et al.'s curve (dotted line) for $T_{\rm eff}$ versus $R-I$ and Taylor's curve (dashed line), versus our data for the K dwarfs (from table 1). Our simple linear fit to the data (Eqn 4) is shown as a solid line. Metal weak stars ([Fe/H] < -1.0 are shown as open squares, showing there is no systematic difference in temperature scale as a function of abundance. The match between the data and the three calibrations is quite satisfactory in the region $0.33 \leq R-I \leq 0.55$. For cooler stars ($R-I \gtrsim 0.55$ i.e. later than about K3) there is a good indication from the Bessell models that our linear fit cannot simply be extrapolated outwards. For stars later than about K3 obtaining accurate abundances from high dispersion spectra becomes increasingly difficult because of the increasing effects of molecular opacity, and it was for this reason that the Morell sample stopped at K3. Stellar atmosphere models and line lists are rapidly improving for cooler stars however, and it should soon be possible to obtain the spectroscopic abundances necessary to extend the calibration to cooler stars still.

In figure 3 we show abundances $[{\rm Fe/H}]_{\rm Gen}$ derived using Eqn. 5 from the $b_1, R-I$ photometry versus the spectroscopically determined abundances $[{\rm Fe/H}]_{\rm Spec}$ for the stars. The scatter is 0.18 dex.

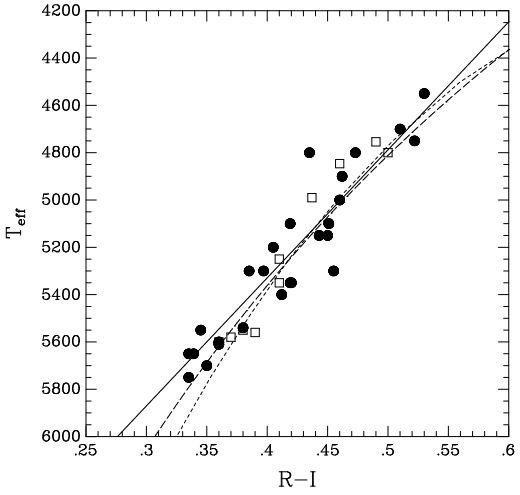

Figure 2. $T_{\rm eff}$ versus $R-I$. The solid line shows our least squares fit (Eqn. 4), the dotted line the Bessell, Castelli and Plez (1996) relation based on synthetic spectra, and the dashed line the Taylor (1992) relation based on analysis of Balmer line wings. Open symbols are stars with [Fe/H]< -1.0.

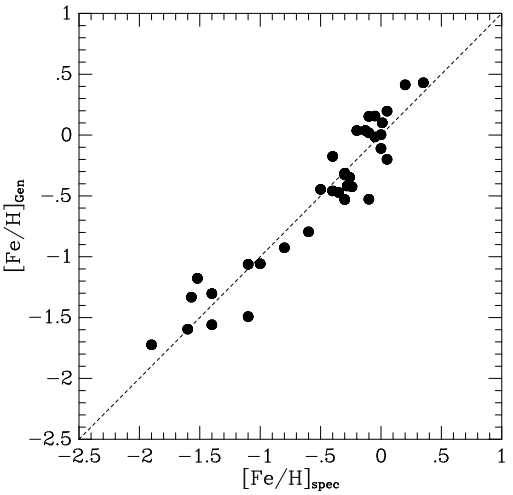

Figure 3. Our final abundance calibration, showing the photometric abundances $[{\rm Fe/H}]_{\rm Gen}$ versus the spectroscopic abundances $[{\rm Fe/H}]_{\rm Spec}$ (calculated using Eqn 5). The line is the 1:1 relation. The scatter for the transformation is 0.18 dex.

3.1 A check using the Hyades

A check of our calibration was made by gathering from the literature Geneva and VRI photometry for G and K dwarfs in the Hyades cluster. Cousins $R-I$ colours going well down the main sequence of the Hyades are available from Reid (1993), and a table of the stars, their broadband colours and Geneva b_1 colour is shown as Table 2. Figure 4(a) shows the colour magnitude diagram in V versus $R-I$ for the Hyades G and K dwarfs. For each star the abundance was estimated

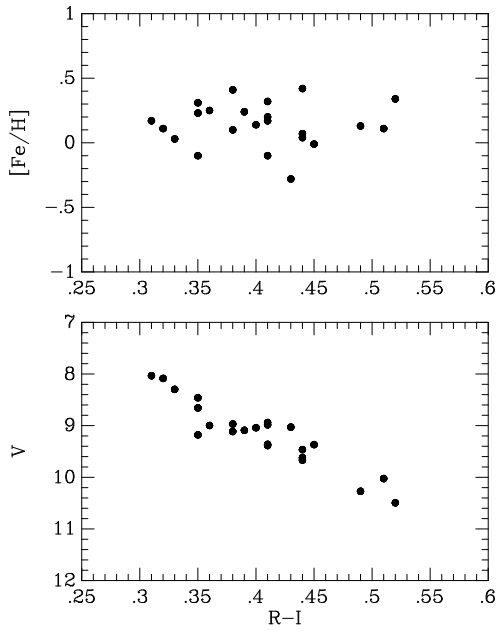

Figure 4. The lower panel shows Hyads in the V versus $R-I$ plane. The upper panel shows the abundance estimate for each star as a function of $R-I$ colour. The mean abundance for the stars is [Fe/H] $= 0.14 \pm 0.03$, with a scatter around the mean of 0.17 dex, representing the error in an individual measurement.

Table 2. Hyades G and K dwarfs.

Name	Sp	V	$R-I$	b_1	$[\mathrm{Fe/H}]_{\mathrm{Gen}}$
BD +20 598	(G5)	9.37	0.45	1.283	−0.01
BD +26 722	(G5)	9.18	0.35	1.166	0.31
HD 26756	G5V	8.46	0.35	1.117	−0.10
HD 26767	(G0)	8.04	0.31	1.087	0.17
HD 27771	K1V	9.09	0.39	1.220	0.24
HD 28099	G8V	8.09	0.32	1.095	0.11
HD 28258	K0V	9.03	0.43	1.219	−0.28
HD 28805	G8V	8.66	0.35	1.157	0.23
HD 28878	K2V	9.39	0.41	1.246	0.20
HD 28977	K2V	9.67	0.44	1.274	0.04
HD 29159	K1V	9.36	0.41	1.243	0.17
HD 30246	(G5)	8.30	0.33	1.101	0.03
HD 30505	K0V	8.97	0.38	1.225	0.41
HD 32347	(K0)	9.00	0.36	1.174	0.25
HD 284253	K0V	9.11	0.38	1.188	0.10
HD 284787	(G5)	9.04	0.40	1.223	0.14
HD 285252	(K2)	8.99	0.41	1.261	0.32
HD 285690	K3V	9.62	0.44	1.320	0.42
HD 285742	K4V	10.27	0.49	1.362	0.13
HD 285773	K0V	8.94	0.41	1.210	−0.10
HD 285830	—	9.47	0.44	1.277	0.07
HD 286789	—	10.50	0.52	1.434	0.34
HD 286929	(K7)	10.03	0.51	1.391	0.11

using Eqn 5, and is shown in column 6 in table 2. The abundances are plotted against the $R-I$ colour in Figure 4(b). The mean abundance of the stars is [Fe/H] $= 0.14 \pm 0.03$ whit a dispersion of 0.17 dex, representing the error in an individual measurement. Taylor (1994) summarises the literature on the Hyades abundance and gives a best estimate of [Fe/H]$= 0.11 \pm 0.01$, so our mean abundance of 0.14 ± 0.03 dex is quite satisfactory. We also note that there is no indication of a trend of derived Hyades abundances as a function of $R-I$ colour, so that for these metal rich stars the temperature-colour relation appears satisfactory.

4 ABUNDANCES AND KINEMATICS OF GLIESE G AND K DWARFS

The Gliese catalog contains around 800 dwarfs classified between G0 and K3 and estimated to be within 25 pc of the Sun. As a pilot study for what will be possible after the *Hipparcos* data are available, we have determined abundances for a subset of these stars having absolute magnitude and space velocity data in the Gliese catalog and photometric data available in the literature. The sample presented here is therefore somewhat inhomogeneous, but the kinematic and abundance properties of the sample nevertheless allow us to compare to previous work on G dwarfs using other (abundance estimation methods) and to show that the G dwarf problem probably extends to the K dwarfs.

We obtained the 1991 version of the Gliese catalog ("Preliminary Version of the Third Catalogue of Nearby Stars" Gliese and Jahreiß) from the Centre de Données astronomiques de Strasbourg and matched up objects with Bessell's (1990) catalog of $UBVRI$ photometry for Gliese stars. We selected stars in $0.33 \leq R-I \leq 0.55$, the colour range of the abundance calibration. For all these stars b_1 data were obtained from the Geneva catalog. Some care was needed when matching the $UBVRI$ and Geneva photometry for stars which were members of multiple systems to be sure the right components were matched; all doubtful cases were excluded from further consideration. Our final lists (184 stars) contained $UBVRI$ and Geneva photometry, parallax and absolute magnitude data, as well as U, V and W velocities for each star. (Here U, V and W are the usual space motions of the star respectively toward the galactic center, the direction of galactic rotation and the north galactic pole.) Abundances for the stars were derived from the $R-I$ and b_1 data using Eqn 5.

Figure 5 shows a colour magnitude diagram for the stars: absolute visual magnitude M_V versus $R-I$ colour, covering approximately G0 to K3. The solid lines show the positions of the main sequence and the giant branch in this plane. Giants and dwarfs have been separated using the dashed line (i.e. $M_V = 4.35$ and $0.33 \leq R-I \leq 0.55$).

There are a number of stars up to 2 magnitudes below the main sequence seen in the diagram. While such stars would classically be termed subdwarfs, the recent results from the 30 month solution for *Hipparcos* (H30 – Perryman et.al. 1995) show that the status of these objects is now uncertain. In fact, most of the objects below the main sequence are not seen at all in H30 (Perryman et al. their Figs. 8 (a) and (b)). Perryman et al. ascribe "a combination of improved parallaxes, and improved colour indices, the in-

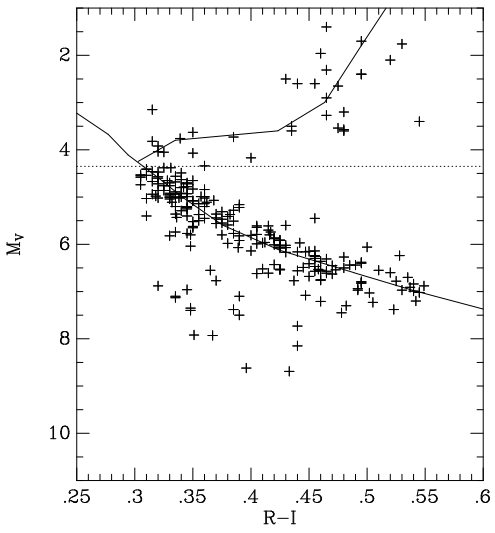

Figure 5. Colour magnitude diagram for the Gliese G and K stars. The positions of the main sequence and giant branch are shown. The dotted line indicates our division into giants (above) and dwarfs (below) using $M_V = 4.35$

fluence of the latter being particularly important" as the possible cause. ⋆ In addition, the H30 results indicate that about two thirds of the stars in the Gliese catalog are not actually within 25 pc, so that we can expect some changes within Figure 5 after the *Hipparcos* data become available. The data for most of the G and K dwarfs analysed here are nevertheless of good quality, and we examine their kinematic and chemical properties next.

In Figure 6 we show the U, V and W velocities of the stars as a function of [Fe/H], as well as the run of mean velocity $< U >$, $< V >$ and $< W >$ and the velocity dispersions σ_U, σ_V, σ_W. † The figure shows the well recognised properties of the old disk, thick disk and halo as has been seen previously in F and G dwarfs and in K giants (see e.g. Freeman 1987, 1996).

4.1 Old disk stars

The old disk is traced in Figure 6 by stars with [Fe/H]$\gtrsim -0.5$. The trend in the velocity dispersions is a slow increase with decreasing abundance, with a possible jump in velocity dispersion in the thick disk regime $-1 \lesssim$[Fe/H]$\lesssim -0.6$. This behaviour is very similar to that seen in local F and G dwarfs (e.g. Edvardsson et al 1993) and for K giants (e.g. Janes 1979, Flynn and Fuchs 1994). For 142 stars with [Fe/H]> -0.5, $(\sigma_U, \sigma_V, \sigma_W) = (37 \pm 3, 24 \pm 2, 17 \pm 1)$.

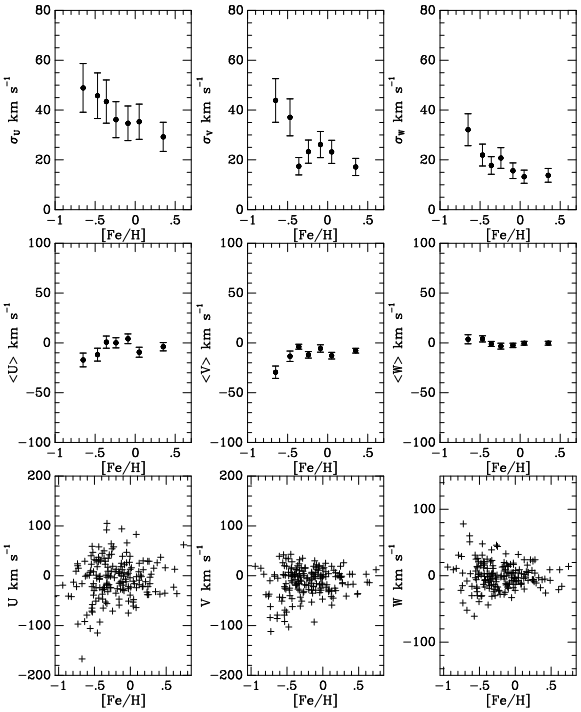

Figure 6. Stellar kinematics of Gliese G and K dwarfs as a function of abundance. Lower panels show the individual velocities in U, V and W as a function of [Fe/H]. Middle panels show the run of mean velocity, and the upper panels the run of velocity dispersion with [Fe/H].

4.2 Thick disk stars

Stars in the range $-1 <$[Fe/H]$\lesssim -0.6$ show a higher velocity dispersion in all three space motions, and can be identified with the thick disk. The ratio of thick disk ($-1 <$[Fe/H]< -0.6) to disk stars ([Fe/H]> -0.5) in the sample is 0.09 ± 0.02, which is the thick disk local normalisation in this volume limited sample. This is in accord with literature estimates of the thick disk local normalisation, which vary between approximately 2 per cent and 10 per cent (Reid and Majewski 1993). The elements of the thick disk velocity ellipsoid‡ $(\sigma_U, \sigma_V, \sigma_W) = (45 \pm 12, 44 \pm 11, 35 \pm 9)$ for 16 stars in the range $-1 <$ [Fe/H]< -0.6, and the assymetric drift is approximately 30 km s^{-1}, all in good accord with previous work (see e.g. Freeman 1987, 1996).

4.3 Metal weak stars

There are 7 stars with [Fe/H] < -1, (two of which are bound to each other, HD 134439 and HD134440 or Gliese 579.2A and B respectively). In a total sample of 184 stars, 7 halo stars seems rather an embarrassment of riches. (Bahcall (1986) estimates the local disk to halo normalisation as

⋆ Our measured abundances and the velocities of these "subdwarfs" indicate that they really are normal disk stars, as H30 appears to show

† The velocities here have been corrected for a solar motion of $U_\odot = 10$ km s^{-1}, $V_\odot = 15$ km s^{-1}and $W_\odot = 8$ km s^{-1}(Kerr and Lynden-Bell 1986)

‡ Note that the star at [Fe/H]$= -0.67, U = -177$ km s^{-1}has been excluded from these calculations, as it may well be a halo interloper

Table 3. Abundance Distributions for G and K dwarfs.

[O/H]	N_G	f_G	N_K	f_K
−1.25	0	0.000	0	0.000
−1.15	0	0.000	1	0.011
−1.05	0	0.000	0	0.000
−0.95	0	0.000	0	0.000
−0.85	0	0.000	0	0.000
−0.75	0	0.000	2	0.023
−0.65	0	0.000	2	0.023
−0.55	0	0.000	2	0.023
−0.45	1	0.010	2	0.023
−0.35	7	0.072	5	0.057
−0.25	28	0.289	13	0.149
−0.15	19	0.196	19	0.218
−0.05	19	0.196	18	0.207
0.05	15	0.155	10	0.115
0.15	6	0.062	7	0.080
0.25	1	0.010	3	0.034
0.35	1	0.010	3	0.034
0.45	0	0.000	0	0.000

The number of G dwarfs, N_G and the number of K dwarfs, N_K binned by [O/H] in bins 0.1 dex wide, where column 1 indicates the bin center. There are 97 G dwarfs and 87 K dwarfs. The relative numbers, normalised to the sample sizes, are shown in the columns headed f_G and f_K. See also Figs 7(b) and (c).

500:1, while Morrison (1993) estimates 850:1). Halo stars are probably over represented in this sample because they are more likely to be targeted for photometric observations. It will be interesting to return to the halo and thick disk normalisations after the *Hipparcos* data are available and we can define and observe a complete volume limited sample of K dwarfs.

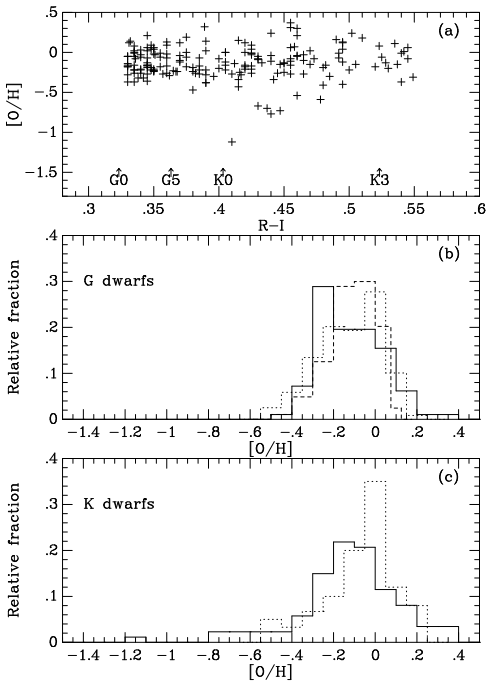

Figure 7. Panel (a) Oxygen abundances for the stars as a function of $R-I$ colour. Panel (b) shows the histogram of [O/H] in the G dwarfs in this sample (solid line), for the Pagel and Patchett (1975) sample (dotted line) and the Rocha-Pinto and Maciel sample (dashed line). Panel (c) shows our [O/H] distribution for the K dwarfs (solid line) and that of Rana and Basu (dotted line).

5 THE METALLICITY DISTRIBUTION

As discussed in the introduction, the metallicity distribution of local G dwarfs has long presented a challenge for explaining the buildup of metallicity in the Galactic disk. We present in this section the abundance distribution for G dwarfs and for K dwarfs using our abundance estimator.

In order to compare to recent work on the G dwarf problem (e.g. Pagel 1989, Sommer-Larsen 1991, Wyse and Gilmore 1995, Rocha-Pinto and Maciel 1996), we convert [Fe/H] to [O/H] using the relations

$$\begin{aligned} [\mathrm{O/H}] &= 0.5[\mathrm{Fe/H}] \qquad [\mathrm{Fe/H}] \geq -1.2 \\ [\mathrm{O/H}] &= 0.6 + [\mathrm{Fe/H}] \qquad [\mathrm{Fe/H}] < -1.2. \end{aligned} \tag{6}$$

When comparing to models, Oxygen abundances are more appropriate because Oxygen is produced in short lived stars and can be treated using the convenient approximation of instantaneous recycling – see e.g. Pagel (1989).

In Figure 7(a) we show the distribution of [O/H] derived using Eqn 6, as a function of $R-I$ colour. The approximate positions of G0, K0 and K3 spectral types are indicated below the stars. Dividing the stars into G and K dwarfs, we show histograms of the stellar abundance in the lower panels, normalised to the sample sizes. In Figure 7(b), the distribution of [O/H] for 97 G dwarfs shows the well known paucity of metal poor stars relative to metal rich stars, i.e the G dwarf problem. The dotted line shows the G dwarf abundance distribution of Pagel and Patchett (1975) and the dashed line the distribution for local G dwarfs of Rocha-Pinto and Maciel (1996). Our histogram follows the previous determinations well, indicating our abundance scale is in good agreement with previous work.

In Fig 7(c) we show the [O/H] distribution for 87 K dwarfs (solid line). Abundance histogram of this type have been determined by Rana and Basu (1990) for F, G and K dwarfs, from the 1984 Catalog of Spectroscopic Abundances (Cayrel de Strobel et al. 1985). This procedure suffers from the shortcoming that the abundance data are inhomogeneous, but we show the abundance distribution of 60 K dwarfs from Rana and Basu by the dotted line in Fig 7(c). Our distribution and that of Rana and Basu are in broad agreement, and are similiar to the abundance distributions for the G dwarfs.

Both the G and K dwarf abundance distributions presented here suffer from selection bias however. Since high proper motion or high velocity stars are frequently targeted for parallax or photometric observations, metal weak stars are likely to be over-represented, as was demonstrated for the halo stars ([Fe/H]< -1) in section 4.3, and even stars with thick disk abundances could be over-represented. Hence, we regard the abundance distributions reported here cautiously, but nevertheless remark that the K dwarf abun-

dance distribution is quite similar to that of the G dwarfs, and offers *prima face* evidence for a "K dwarf problem". The *Hipparcos* data offer the exciting prospect in the near future of defining a large, complete and volume limited sample of G and/or K dwarfs, largely circumventing the above difficulties. Our abundance distributions for the G and K dwarfs are shown in Table 3.

In summary, the kinematics and abundances of the G and K dwarfs examined in this section follow the trends already well established in the solar neighbourhood for F and G dwarfs and for K giants. The ability to measure abundance in K dwarfs offers several interesting possibilities, especially after the *Hipparcos* data become available. As future work, we plan to analyse the metallicity distribution of an absolute magnitude selected and volume limited sample of K dwarfs, which will give us a very clean view of metallicity evolution in the solar cylinder.

6 CONCLUSIONS

We have calibrated an abundance index for G and K dwarfs, which uses broadband Cousins $R-I$ photometry to estimate stellar effective temperature, and the Geneva b_1 colour to measure line blanketing in the blue. Our calibration is based on a recent sample of accurate abundance determinations for disk G and K dwarfs, (Morell, Källander and Butcher 1992 and Morell 1994) determined from high dispersion spectra. The index gives [Fe/H] estimates with a scatter of 0.2 dex for G0 to K3 dwarfs. The [Fe/H] estimator has been checked using the stars in the Hyades cluster, and we derive a mean abundance for the stars of [Fe/H]= 0.14 dex, consistent with previous determinations. We take a sample of G and K dwarfs from the Gliese catalog, find $R-I$ and b_1 data from the literature, and derive the local abundance distribution for approximately 200 G and K dwarfs. The kinematics of the G and K dwarfs are examined as function of abundance, the K dwarfs for the first time, and we see the well known kinematic properties of the local neighbourhood, as established in the literature from studies of F and G dwarfs and from K giants. The abundance distributions in the G and K dwarfs are quite similar, indicating that the "G dwarf problem" extends to the K dwarfs.

ACKNOWLEDGMENTS

We thank Bernard Pagel for many helpful discussions and Helio Rocha-Pinto for interesting comments. This research has made extensive use of the Simbad database, operated at CDS, Strasbourg, France.

REFERENCES

Bahcall J.N., 1986, ARA&A, 24, 577
Cayrel de Strobel G., Bentolila C., Hauck B., Duquennoy A., 1985, A&AS, 59, 145
Cayrel de Strobel G., Hauck B., Francois P., Thevenin F., Friel E., Mermilliod M., Borde S., 1992, A&AS, 95, 273
Bessell M.S., 1990, A&AS, 83, 357
Bessell M.S., Castelli F. and Plez B., 1996, preprint
Carney B. and Petersen R.C., 1980, ApJ, 244, 989
Flynn C. and Fuchs B., 1994, MNRAS 270, 471
Freeman K.C., 1987, ARA&A, 25, 603
Freeman K.C., 1996, in "Formation of the Galactic Halo... Inside and Out", Eds. H. Morrison and A. Sarajedeni, ASP conference Series, Vol. 92, p3.
Gustafsson B., Bell R.A., Eriksson K, Nordlund Å, 1975, A&A, 42, 407
Kerr F. and Lynden-Bell D., 1986, MNRAS, 221, 1023
Gilroy K.K., Sneden C., Pilachowski C.A., Cowan J.J., 1988, ApJ, 327, 298
Morell O., 1994, Ph. D. Thesis, Uppsala University. Acta Universitatis Upsaliensis
Morell O., Källander D. and Butcher H.R., 1992, A&A, 259, 543
Morrison H., 1993, AJ, 106, 578
Pagel B.E.J., 1989, Rev. Mex. Astr. Astrof. 18, 161
Pagel B.E.J. and Patchett, B.E., 1975, MNRAS, 172, 13
Perryman M. A. C., et al., 1995, A&A,304,69
Petersen R.C., 1980, ApJ, 235, 491
Petersen R.C., 1981, ApJ, 245, 238
Rana N.C. and Basu S., 1990, Ap&SS, 168, 317
Rebolo R., Beckman J.E. and Molaro P., 1988, A&A, 192, 192
Reid I.N., 1993, MNRAS, 265, 785
Reid I.N., Majewski, S.R., 1993, ApJ, 409, 635
Rocha-Pinto H.J. and Maciel W.J., 1996, MNRAS, 279, 447
Rufener F., 1989, A&AS, 78, 469
Ryan S., 1992, AJ, 104, 1144
Sneden C. and Crocker D., 1988, ApJ, 335, 906
Sommer-Larsen J., 1991, MNRAS, 249, 368
Spite M. Spite F. and Maillard, J.P., 1984 A&A, 141, 56
Taylor B., 1992, PASP 104, 500
Taylor B., 1995, PASP 107, 734
vanden Berg D.A. and Bell R.A., 1985, ApJS, 58, 561
Wyse R. and Gilmore G., 1995, AJ, 110, 2771